Detection of alternative conformations by unrestrained refinement

Oleg V. Sobolev* and Vladimir Y. Lunin

Laboratory of Macromolecular Crystallography, Institute of Mathematical Problems of Biology, RAS, 4 Institutskaia St., Pushchino 142290, Moscow Region, Russian Federation

Correspondence e-mail: sobolev@impb.psn.ru

Unrestrained refinement is stable for the vast majority of atoms when working at atomic resolution. Nevertheless, geometrical restraints should be retained in refinement for residues that are present in several (alternative) conformations in the crystal used for the X-ray experiment; otherwise, such residues deteriorate significantly. The authors believe that a large distortion of a residue in unrestrained refinement may hint at the presence of alternative conformations of this residue. To obtain these hints in a routine way, two methods of analyzing the shifts of atomic centres resulting from several cycles of unrestrained refinement are described. A simple diagram plotting the values of the atomic shifts against the residue number may give an idea of the crystallographic order of different parts of the structure at a qualitative level. To put the analysis on a more quantitative basis, several decision-making procedures were developed and tested which compose a list of residues that are likely to be present in alternative conformations or to be disordered and so should be checked thoroughly using Fourier syntheses and included in the model with alternative conformations when necessary. The parameters and performance of the suggested procedures were estimated by the use of 203 PDB structures refined at resolutions better than 1.2 Å. Decision-making procedures based on analysis of atomic shifts were found to be more reliable than similar procedures based on atomic displacement parameters or density values calculated at atomic centres.

1. Introduction

In an ideal crystal, the content of different unit cells is assumed to be identical and every amino-acid residue has the same conformation in all copies of the unit cell. However, in real protein crystals different kinds of static and dynamic disorder may be present. In particular, some residues may be present in the crystal in a small number (two or three) of alternative conformations. To model this situation, coordinates of several alternative conformations are included in an atomic model with partial occupancies. Alternative conformations can be detected not only for side chains, but also for parts of the main chain (Howard *et al.*, 2004; Ševčík *et al.*, 2004; Wang *et al.*, 2007). The modelling of alternative conformations increases the accuracy of the calculated structure-factor phases and results in more precise electron-density maps in the whole unit cell. Furthermore, in some cases the possibility of alternative conformations is related to protein function (Rypniewski *et al.*, 2001; Getzoff *et al.*, 2003; Kursula & Wierenga, 2003; Ševčík *et al.*, 2004). It has been noted that the number of residues that can be modelled in alternative conformations increases with the resolution of the experi-

mental data (Addlagatta *et al.*, 2001; Howard *et al.*, 2004; Wang *et al.*, 2007). Detection of residues that are present in alternative conformations is time-consuming and demands visual analysis of electron-density maps by an experienced crystallographer. The goal that we address in this study is to develop a method that could help in the search for residues that are present in alternative conformations in the studied crystal.

Generally, a target function for crystallographic refinement of biological macromolecules consists of two parts. The first part of this criterion ensures correspondence between the model and X-ray data. The second part of the criterion places restraints on model geometry. The presence of the second part compensates for the relatively low data-to-parameter ratio and stabilizes refinement. Refinement without stereochemical restraints is unstable at low and medium resolutions; nevertheless, well ordered parts of the structure can be refined without stereochemical restraints in the last steps of refinement if the resolution of the experimental data is sufficiently high (Dauter *et al.*, 1992; Dodd *et al.*, 1995; Koepke *et al.*, 2003). Sometimes it is even possible to refine the whole structure without stereochemical restraints (Getzoff *et al.*, 2003). It was noted long ago that even at atomic resolution poorly ordered residues deteriorate significantly during unrestrained refinement, while ordered residues are stable (Dauter *et al.*, 1992).

In this paper, we discuss to what extent the deterioration of a residue in high-resolution unrestrained refinement can be used as an indicator to detect alternative conformations. The suggested approach consists of several cycles of unrestrained refinement followed by calculation and analysis of the values of the shifts of atoms resulting from this refinement. We suggest two approaches to the analysis of the shifts. The first is the visual analysis of a diagram of atomic shifts *versus* residue number. The largest shifts indicate the residues that are considered in this approach as the main candidates to be present in alternative conformations and that should be checked first. This approach has been tested previously by selective analysis of several structures (Sobolev, 2008; Sobolev & Lunin, 2008) and has shown promising results. We discuss this approach briefly in §2.2.

The second approach presents a type of automated decision-making procedure that classifies every residue as 'single conformation' (SC) or 'alternative conformations' (AC). The procedure is based on the observation that SC residues and AC residues have different mobilities in unrestrained refinement. The decision is made either by comparing the observed atomic shifts with a predetermined threshold or by comparing the probabilities of such shifts for SC and AC residues. To study the mobility of different kinds of residues in unrestrained refinement and to derive procedure parameters, an analysis of a large number of protein structures stored in the Protein Data Bank (Berman *et al.*, 2000) was conducted. The suggested decision-making procedures may be considered as binary classification statistical tests. Standard statistical approaches were applied to evaluate their efficiency.

In this work, the basic resolution was chosen as 1.2 Å as it seems that this is the limiting value for a successful unrest-

rained refinement. This limit coincides with an empirical rule formulated by Sheldrick (1990) that it is very unlikely that a structure can be solved using direct methods if the resolution of the X-ray data is worse than 1.2 Å. Evidence for this rule has been discussed by Morris & Bricogne (2003). The performance of the decision-making procedures at higher and lower resolutions is discussed briefly in §4.4. A similar statistical analysis was performed for decision-making procedures based on atomic displacement parameters (B factors) and on the values of Fourier syntheses calculated at atomic centres (see §4.5).

It should be noted that like other statistical tests the proposed procedures do not guarantee the correctness of the decision; they just highlight the residues that must be most carefully checked using Fourier syntheses.

2. Methods

2.1. TUR routine

To analyze a particular model, we apply the trial unrestrained refinement (TUR) routine. The routine consists of several cycles of unrestrained refinement followed by calculation of the shift of each atom, *i.e.* the distance between the positions of the centre of the atom before and after refinement. The set of atomic shifts forms the output of the TUR. This output may be used to visualize TUR results or to generate in an automated mode a list of problematic parts of the model that should be checked. In our studies, the trial refinement consisted of three macrocycles of unrestrained refinement with the *phenix.refine* program.

2.2. Visual analysis of atomic shifts

Visually, the TUR results can be displayed as a diagram presenting atomic shifts *versus* residue number (Fig. 1). In this diagram, each dot corresponds to one non-H atom and dots corresponding to the same residue are grouped in columns. High columns reveal residues that had significant atomic shifts in unrestrained refinement and thus are unstable and are
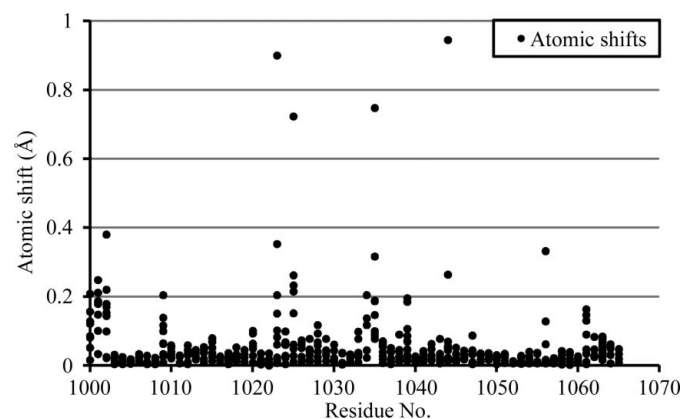

Figure 1
The output of TUR for PDB entry 1hg7 (Antson *et al.*, 2001). Each column of dots represents the shifts of non-H atoms in one of the residues. The residues are numbered as in the PDB file.

suspected to be present in alternative conformations. The diagrams can be plotted separately for main-chain and side-chain atoms (Fig. 2); this can simplify the search for unstable parts of the main chain. The diagram provides a hint to which residues may have alternative conformations, but the proper choice of cutoff level for the selection of high columns is not always obvious.

2.3. Automation of analysis of atomic shifts

To classify every residue as 'single conformation' (SC) or 'alternative conformations' (AC) in an automated mode, several decision-making procedures were developed and tested. These procedures have a common basis, but differ in the details. Each procedure uses the TUR results to generate a list of residues suspected of being present in alternative conformations.

2.3.1. Integral measure of residue deterioration. In the TUR, each atom receives an individual shift. To discuss alternative conformations in terms of residues, it is sometimes convenient to use some integral measure that reflects the mobility of a group of atoms (*e.g.* main-chain or side-chain atoms of a particular residue). In this paper, we use two such measures, namely the average shift and the maximal shift calculated for atoms belonging to some group.

2.3.2. Threshold-based decision criteria. The simplest way to form a list of potential AC residues is to compare the integral shift value of each residue obtained in the TUR with some threshold value. If the integral shift value is greater than the threshold, then the residue is classified as an AC residue. If the integral shift value is smaller than the threshold, then the residue is classified as an SC residue. The threshold value is a parameter of the decision-making procedure and it may be adjusted to give the best prediction quality. It should be noted that different kinds of atoms (*e.g.* side-chain and main-chain atoms) may have different mobilities in unrestrained refinement. Therefore, threshold values may be set differently for different kinds of atoms.
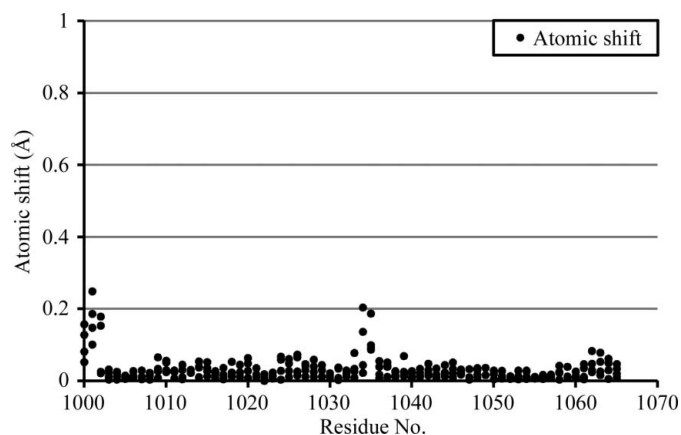

Figure 2
The output of TUR for main-chain atoms of PDB entry 1hg7 (Antson *et al.*, 2001). Each column of dots represents the shifts of non-H atoms in one of the residues. The residues are numbered as in the PDB file.

Table 1
Database statistics.

	Database 1	Database 2
Conditions		
Resolution limits (Å)	$1.1 \leq d \leq 1.2$	$d < 1.1$
R-factor limits		
Maximum R_{work}	0.13	0.12
Maximum R_{free}	0.16	0.15
Statistics		
Structures selected from the PDB	189	102
Structures prepared for tests	135	68
Non-H atoms in the database	334985	140185
Atoms in AC in the database	20510	16457

2.3.3. Likelihood-based decision criteria. Another type of procedure was based on the maximum-likelihood principle. In this approach, we used two probability distributions for the integral shift value. The first distribution corresponded to the SC residues and the second to the AC residues. These distributions were derived empirically using the database described below in §2.4. The distributions may be different for different kinds of atoms (§3.2). To make a decision concerning a particular residue, the integral shift value was calculated as well as the probability of obtaining this value for the SC residue case and for the AC residue case. If the probability is larger for the AC case, then the residue is classified as an AC residue. Otherwise, it is classified as an SC residue.

As one further modification of a likelihood-based approach, the likelihood was calculated as the probability of obtaining a whole set of atomic shifts instead of the probability of obtaining the obtained integral value of the shifts. This probability was calculated as the product of the probabilities of individual shifts using empirical distributions corresponding to individual atomic shifts.

2.4. Preparing of databases of atomic shifts

2.4.1. Selection of PDB models. To study the mobility of atoms in unrestrained refinement and to derive parameters for decision-making procedures, two databases were composed corresponding to two different resolution zones. The first database corresponded to resolutions between 1.1 and 1.2 Å and the second database corresponded to resolutions better than 1.1 Å. Other conditions are listed in Table 1. We set limits on the *R*-factor values of the selected models to choose high-quality structures which had been studied carefully so that the alternative conformations were assigned reliably.

2.4.2. Preparing models. The process of preparing the database consisted of three stages, namely model preparation, trial unrestrained refinement and analysis of atomic shifts. The goal of the first stage was to 'restore' the model as it would have been before alternative conformations were included. For this purpose, only the conformation possessing the largest occupancy was left in the model for each residue, with the occupancies set to 1. Structure-factor magnitudes extracted from the PDB were converted to MTZ format with the *phenix.cif_as_mtz* program from the *PHENIX* package (Adams *et al.*, 2010), H atoms were included with *phenix.ready_set* and geometry restraints for nonstandard

ligands were built with *phenix.elbow* (Moriarty *et al.*, 2009). Standard restrained refinement was performed for this model with *phenix.refine* (Afonine *et al.*, 2012) using anisotropic ADPs and riding H atoms. In the second stage, TUR consisting of three macrocycles was performed for this model with *phenix.refine*. In the third stage, we calculated atomic shifts after TUR for all atoms. Owing to the large number of selected models, we used an automated processing procedure. This procedure failed to process some of the selected models at different stages of preparation. The main reasons for these failures were an inability to automatically convert CIF files to MTZ format or an inability to automatically produce a CIF file for a ligand with *phenix.elbow*. Some of the refinements ended with rather high *R*-factor values after the first stage. Structures with R_{work} values greater than 0.16 and 0.15 were excluded from the first and second databases, respectively. Nevertheless, the number of models that were processed successfully was sufficient to continue the research.

2.4.3. Composing databases. The atomic shifts resulting from the unrestrained refinement were calculated and included into the databases together with information identifying the atom (PDB code of the structure, residue and atom types) and some complementary information: the alternate location indicator, the solvent accessibility of the corresponding residue, the *R* factor, the ADP and the value of the electron density at the atom centre in the weighted $2mF_{obs} - DF_{calc}$ Fourier synthesis calculated in the first stage of model preparation. The solvent accessibility was calculated using the *DSSP* program (Kabsch & Sander, 1983). In our study, we considered residues with accessibility greater or equal to 50 as belonging to the surface of the molecule. The density values in combined Fourier syntheses were calculated with *phenix.model_vs_data* (Afonine *et al.*, 2010).

2.5. Testing of the decision-making procedures

2.5.1. Statistical criteria for evaluating decision-making procedures. The decision-making procedures discussed above may be considered as binary classification statistical tests and
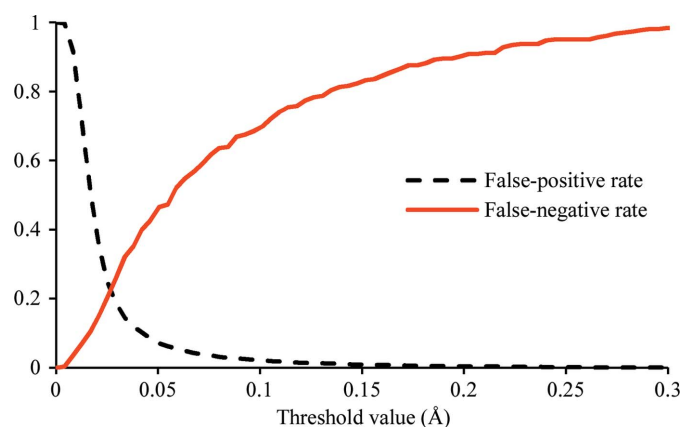

Figure 3
False-positive and false-negative rates *versus* threshold value for the threshold criterion based on the mean shift for the class of side inner chains (test sample, database 1, $0.0961 \leq R_{work} \leq 0.1278$).

standard statistical approaches may be applied to estimate their quality. To adjust the parameters of the procedures and to evaluate their performance, each of the two databases was divided into two equal parts. The first part (training sample) was used to find appropriate cutoff levels and to calculate empirical distributions of the shifts. The second part (test sample) was used to evaluate the quality of the procedures, supposing the PDB assignments of SC or AC to be the 'true answers' (see discussion in §4.1). For a particular residue, we consider the result of the test as positive if the decision-making procedure gives the prediction 'the residue is present in AC' and as negative if the prediction is 'the residue is present in an SC'. We assume that the procedure gives a true prediction if the result matches the structure deposited in the PDB, *i.e.* either the criterion indicates the presence of AC and the model deposited in the PDB does contain alternative conformations for the residue or the procedure indicates SC and this residue is present in the model in a single conformation. Other variants are considered as false answers of the procedure. We assume that a residue has alternative mainchain or side-chain conformation if it has at least one AC atom in the chain. Alanine and glycine residues were excluded from evaluation of the quality of the side-chain prediction.

The two main characteristics that are used to evaluate the quality of the statistical test are the 'false-positive rate' (fp_rate) and the 'false-negative rate' (fn_rate). In our case, fp_rate indicates the fraction of residues that were detected as AC while they are present in only one conformation in the PDB. fn_rate indicates the fraction of residues that were classified as SC while in the PDB they are present in several alternative conformations. In our study, fp_rate and fn_rate were estimated from the test sample as

$$
\begin{aligned}
\mathrm{fp\_rate} &= \frac{\mathrm{FP}}{\mathrm{TN} + \mathrm{FP}}, \\
\mathrm{fn\_rate} &= \frac{\mathrm{FN}}{\mathrm{TP} + \mathrm{FN}}.
\end{aligned} \tag{1}
$$

Here, TP is the number of correctly predicted AC (true positive), TN is the number of correctly predicted SCs (true negative), FP is the number of incorrect AC predictions (false positives) and FN is the number of incorrect SC predictions (false negatives). Fig. 3 shows the two rates *versus* the threshold value for the threshold-based criterion applied to the mean shift for the class of side inner chains (see §3.2.2).

The two curves shown in Fig. 3 may be combined into one receiver-operating characteristic (ROC) curve (Fig. 4). Every point on this ROC curve corresponds to some threshold value and has coordinates equal to the corresponding fp_rate and $(1 - \mathrm{fn\_rate})$ values. The value $(1 - \mathrm{fn\_rate})$ is called the 'true positive rate'. It may be calculated from the database as

$$
\mathrm{tp\_rate} = \frac{\mathrm{TP}}{\mathrm{TP} + \mathrm{FN}}. \tag{2}
$$

The curve shows the dependence of a 'benefit' (the proportion of AC present which were correctly predicted as alternative) on a 'cost' (the proportion of SCs present which we wrongly predicted as AC). A good decision-making procedure should

find a large percentage of AC residues (tp_rate) at the cost of a low rate of false alarms (fp_rate). The ROC curve allows an estimation of the extent to which this is possible. The evaluation of the quality of a likelihood-based criterion may be reflected as the single point with coordinates (fp_rate, tp_rate) in ROC space.

There are two further values that can be useful for the evaluation of statistical criteria, namely the positive predictive value (PPV) and the negative predictive value (NPV),

$$PPV = \frac{TP}{TP + FP},$$
$$NPV = \frac{TN}{TN + FN}. \quad (3)$$

In our case, the PPV gives the share of correct predictions among all AC predictions and the NPV gives the share of correct predictions among all SC predictions.

2.5.2. Summary characteristics of statistical tests. In threshold-based statistical tests, the values of fp_rate and fn_rate are competitive values and depend on the threshold value. A similar observation is also valid for PPV and NPV. As a compromise, a single-value measure of goodness can be defined as the 'balanced accuracy' (bACC),

$$bACC = \frac{(1 - fp\_rate) + (1 - fn\_rate)}{2} \quad (4)$$

as suggested previously in CASP competitions devoted to 'identifying disordered regions in target proteins' (Noivirt-Brik *et al.*, 2009). In threshold-based procedures bACC depends on the threshold value and the choice of threshold may be optimized to obtain the maximal possible balanced accuracy.

Another considered summary value is the area under curve (AUC) calculated for the ROC curve. This value is calculated for the threshold-based procedures. A large value of this area
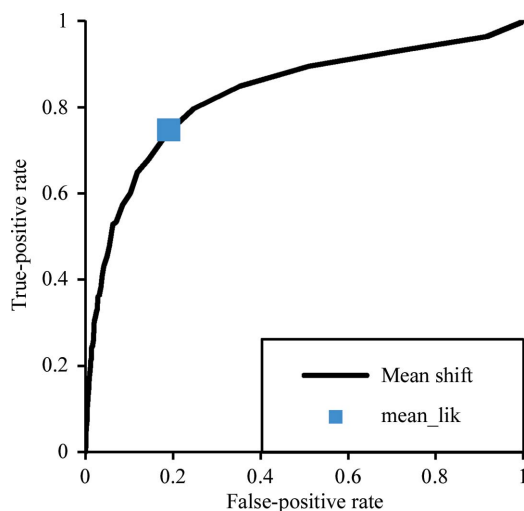
means that we can choose a threshold that results in small probabilities of both types of errors simultaneously. In our study, the AUC value is equal to the probability of having a larger shift value for an AC residue than for an SC residue if these two residues are chosen randomly (Fawcett, 2006).

3. Results

3.1. Diagrams of atomic shifts

Fig. 5 shows an example of a diagram plotted for PDB entry 1hg7 (Antson *et al.*, 2001). The markers in this figure highlight the residues for which the authors of the structure introduced AC. The colour of the marker indicates the refined value of the occupancy for the conformation with lower occupancy. It is easy to see that in general AC were introduced for residues that had significant atomic shifts in the unrestrained refinement. Moreover, AC with near to equal occupancies were found for residues that revealed larger atomic shifts in comparison with residues possessing minor occupancy (*e.g.* 0.3) for one of the alternative conformations. On the other hand, some residues possessing AC in the PDB model were not revealed by large atomic shifts.

3.2. Atomic mobility in unrestrained refinement

Analysis of the atomic shifts obtained in the unrestrained refinement revealed different mobilities for different kinds of atoms. These distinctions were taken into account when constructing decision-making procedures; the threshold values and the probability distributions for atomic shifts were defined differently for different kinds of atoms.

3.2.1. Single- and alternative-conformation types of atoms. All atoms in the database may be divided into two types, namely SC atoms, which are atoms that have unique coordinates in the PDB model, and AC atoms, which have multiple
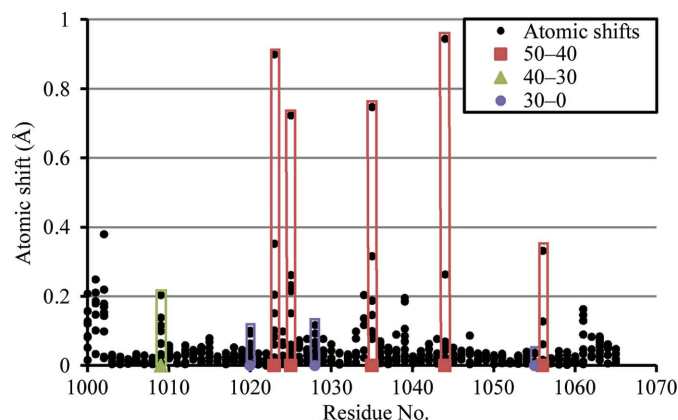
Figure 4
ROC curve for the decision-making procedure based on the mean shift. The curve corresponds to the class of 'side inner' residues (test sample, database 1, $0.0961 \leq R_{work} \leq 0.1278$). The square marker shows the quality of the procedure based on the likelihood of the mean shift (mean_lik).

Figure 5
The output of TUR for PDB entry 1hg7 (Antson *et al.*, 2001). Each column of dots represents the shifts of non-H atoms in one of the residues. The residues are numbered as in the PDB file. Markers and rectangles indicate the residues that were defined by the authors as AC residues. The colours and shapes of the markers reflect the refined values of the occupancies for the less populated conformations.

Table 2
The balanced accuracy values (bACC) for decision-making procedures (database 1, test sample).

Classes: MI, main inner; MO, main outer; SI, side inner; SO, side outer; M, all main; S, all side (see §3.2.2).

Criterion type	Atom classes					
	MI	MO	SI	SO	M	S
Mean_shift	0.631	0.591	0.776	0.719	0.611	0.760
Max_shift	0.642	0.595	0.765	0.713	0.616	0.745
Mean_shift_lik	0.560	0.585	0.765	0.701	0.602	0.764
Max_shift_lik	0.592	0.582	0.732	0.693	0.586	0.734
Shift_lik	0.603	0.588	0.754	0.700	0.600	0.741

coordinate records in the PDB file. Fig. 6 shows empirical distributions of atomic shifts for these two types of atoms.

These distributions are different and form the basis for distinguishing atom types by study of their shifts in TUR. The distribution of atomic shifts for SC atoms has a sharper peak which is situated on the left-hand side of the graph. The peak for AC atoms is smeared.

3.2.2. Atom classes. One can expect that side chains will normally be less ordered than the main chain in a crystal and that residues exposed to the solvent will be less ordered than residues lying in the molecular core. This may result in different mobilities of atoms in unrestrained refinement even when atoms are present in a single conformation. To take this effect into account, the atoms were divided into four classes, namely 'main inner' (MI), 'main outer' (MO), 'side inner' (SI) and 'side outer' (SO), and the distributions of shifts were calculated separately in these classes. Fig. 7 shows the mean atomic shifts for these four classes of atoms. As expected, the atomic shifts for main-chain atoms are smaller on average than those for side-chain atoms and the shifts for core residues are smaller than those for surface residues.

3.2.3. R-factor-based batches. Crystallographic R factors reflect the overall quality of the model. A relatively large value of the R factor may mean that refinement of the model has not been completed or may be caused by enhanced disorder of the crystal. In both cases it is natural to expect
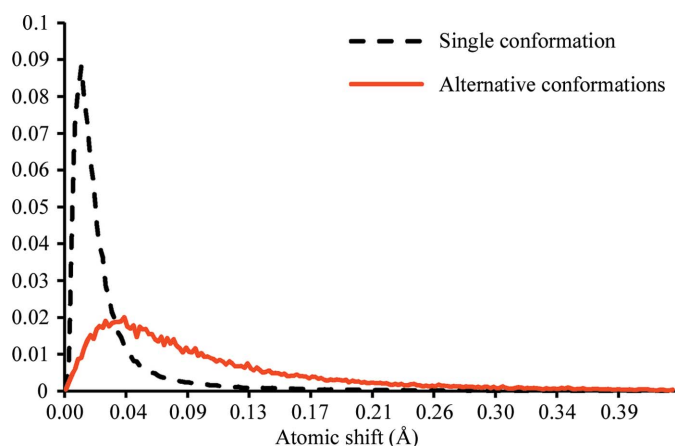
Table 3
The area under the ROC curve (AUC) for threshold-based decision-making procedures.

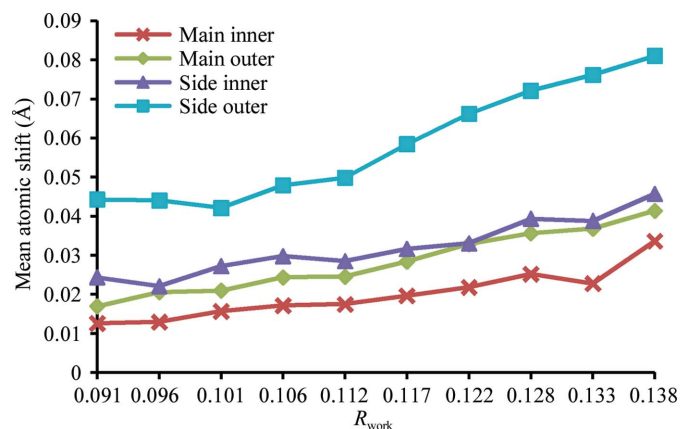Database 1, test sample, $0.0961 \leq R_{work} \leq 0.1278$.

Criterion type	Atom classes			
	MI	MO	SI	SO
Mean_shift	0.606	0.587	0.851	0.779
Max_shift	0.611	0.587	0.835	0.767

increased mobility of atoms in unrestrained refinement. Fig. 7 confirms this expectation. In all of the classes the mean shift of atoms in TUR increases with the final value of the R factor. To take this effect into account, the atoms in the classes were additionally divided into several batches in accordance with the R-factor value corresponding to the whole model before TUR.

3.3. Evaluation of decision-making procedures

Five decision-making procedures were organized as described in §2.3 with the use of individual threshold values and probability distributions adapted for different kinds of atoms (see §3.2). The procedures differ by the type of integral shift value (mean or maximum) and the type of decision criterion (threshold or likelihood-based). The thresholds and distributions were derived using the training sample of the corresponding database. The threshold values were adapted to maximize the corresponding bACC values on the basis of the training samples. The results of evaluation of the suggested decision-making procedures on the basis of test samples are shown in Tables 2 and 3.

Tables 4 and 5 show the results of evaluation of the mean shift threshold-based criterion for different resolutions. The results of evaluation of the four other criteria are omitted as they showed no significant differences from the presented results. Fig. 8 presents ROC curves corresponding to four classes of residues. The errors obtained for likelihood-based criteria and the best threshold choice are indicated by markers.

Figure 6
Distributions resulting from TUR atomic shifts for SC (black dashed line) and AC (red solid line) types of atoms (database 1).

Figure 7
Mean shifts of SC atoms in unrestrained refinement *versus* the R factor. The values are calculated separately for four different atom classes (database 1).

Table 4
Evaluation of mean-shift threshold-based criteria for database 1 (1.1–1.2 Å), test sample.

See equations (1), (3) and (4) for definitions.

Atom class	bACC	fp_rate	fn_rate	PPV	NPV	Fraction of AC
Main inner	0.631	0.244	0.495	0.052	0.983	0.027
Main outer	0.591	0.278	0.540	0.104	0.950	0.070
Side inner	0.776	0.212	0.236	0.181	0.982	0.061
Side outer	0.719	0.365	0.196	0.281	0.948	0.178
Main (overall)	0.611	0.256	0.521	0.073	0.971	0.042
Side (overall)	0.760	0.270	0.211	0.235	0.970	0.105

Table 5
Evaluation of mean-shift threshold-based criteria for database 2 ($d <$ 1.1 Å), test sample.

See equations (1), (3) and (4) for definitions.

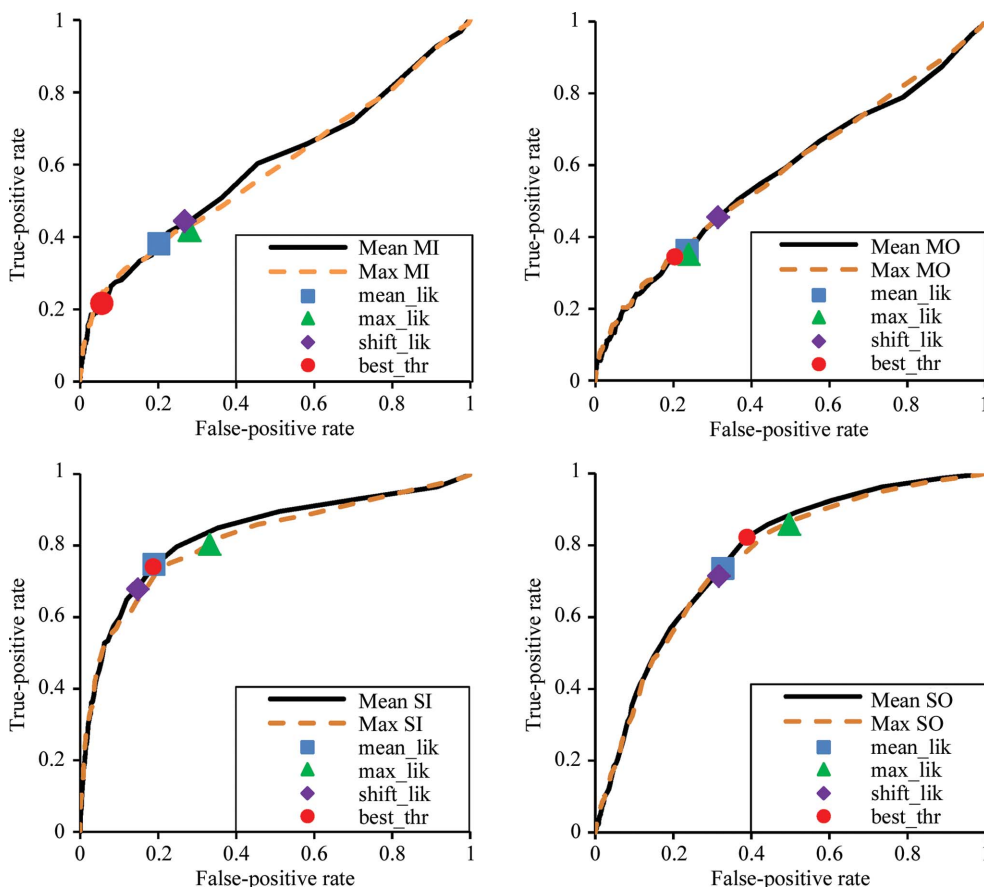| Atom class	bACC	fp_rate	fn_rate	PPV	NPV	Fraction of AC
Main inner	0.661	0.164	0.512	0.176	0.958	0.071
Main outer	0.666	0.373	0.295	0.210	0.938	0.141
Side inner	0.781	0.130	0.308	0.389	0.959	0.119
Side outer	0.735	0.245	0.285	0.515	0.880	0.363
Main (overall)	0.681	0.237	0.401	0.195	0.952	0.096
Side (overall)	0.768	0.170	0.293	0.460	0.932	0.205

Figure 8
Evaluation of decision-making procedures (database 1, test sample, $0.0961 \leq R_{\text{work}} \leq 0.1278$) for different atom classes (MI, MO, SI and SO as defined in §3.2.2). Solid and dashed lines correspond to mean-shift (mean) and maximum-shift (max) threshold-based criteria, respectively. Squares, triangles and diamonds correspond to criteria based on the likelihood of mean (mean_lik) and maximum (max_lik) shifts and individual shifts of atoms (shift_lik). The circle (best_thr) marks the optimal threshold value corresponding to the mean-shift criterion.

4. Discussion

4.1. Reliability of databases

The aim of this study was to determine whether analysis of the mobility of atoms in trial unrestrained refinement (TUR) can be used to identify residues with alternative conformations in the crystal. Based on this study, several procedures have been proposed for predicting the availability of alternative conformations for particular residues. The proposed procedures generate a list of residues that are most likely to have alternative conformations in the crystal used and thus should be inspected first with electron-density maps.

It should be noted that careful study of the proposed decision-making procedures indicates some difficulties that affect the reliability of the results and that have not yet been overcome. Firstly, the behaviour of atoms in unrestrained refinement may be affected by many factors, so the presence of alternative conformations is not the only reason for the distortion of a residue. Next, to adjust decision-making procedure parameters and evaluate procedure quality we need some training and test samples with known true answers. In our study we rely on the opinions of the authors who deposited the structures in the PDB, but their decisions may sometimes be questionable. The presence of an alternative conformation for a residue may be a disputable issue, even when electron-density maps are analyzed thoroughly. Usually, the decision to include an alternative conformation in the model is confirmed by this analysis, while a single conformation is supposed by default. As a consequence, the number of residues possessing alternative conformations seems to be underestimated in the PDB. This introduces noise in the SC samples, since they contain wrongly included residues that are actually present in alternative conformations. As a result, the corresponding empirical probability distributions reveal artificially high probabilities for large shifts, and the threshold values in threshold-based approaches are too high. This results in a partial loss of AC residues in the output list and increases the number of negative faults in the procedure-evaluation stage. On the other hand, this leads to an increase in the number of positive faults, since some correctly identified AC residues are classified as 'false

positives' in the evaluation procedure because they are wrongly marked as SC residues in the database. Finally, at the present time we are unable to distinguish between residues present in AC and fully disordered residues.

A possible way to overcome these difficulties could be to use a database composed of a small number of precisely studied structures, but this approach also has drawbacks. Firstly, it is extremely time-consuming and only a small number of structures can be analyzed in this way within a reasonable time. Therefore, such a database would contain a very small number of structures. Note that this analysis should be at least as thorough as the analysis performed by the original authors. The second issue is the ambiguous interpretation of ill-defined areas in electron-density maps. The experts may sometimes have opposing opinions about the necessity of introducing alternative conformations for a particular residue. In our study, we have used a larger database based on the assignments of the authors of the PDB entries, but with the necessary caution when using the results of predictions.

4.2. Atomic mobility in unrestrained refinement as a basis for the detection of alternative conformations

The first part of this research was devoted to the study of atomic mobility in unrestrained refinement. As one might expect, this analysis revealed that side-chain atoms usually have larger shifts than main-chain atoms and that atoms on the surface of the molecule have larger shifts than atoms inside the globule. Similarly, the expected difference in mobility was found for atoms occupying alternative positions in the crystal in comparison with those possessing a unique position. This difference formed the basis of the suggested method for the detection of alternative conformations. Less expected (but not surprising) is the dependence of atomic mobility on the overall structure quality. Structures with relatively high R factors demonstrated increased atomic mobility, which may mean that the refinement process had not been completed. The results of the analysis were further used to fine-tune the suggested decision-making procedures. It is worth noting that although only high-quality structures were used to estimate procedure parameters, the developed procedures can then be applied to any studied structure.

4.3. Automatic decision-making procedures for the detection of alternative conformations

Testing of the automatic decision-making procedures showed that, as expected, the results are statistical in nature and contain errors of both types (false positives and false negatives). The prediction quality achieved is different for different parts of a structure. The best predictions were obtained for side chains situated inside the globule and those for surface side chains were slightly worse. Much worse results were obtained for main-chain atoms. The worse results for main-chain atoms can be explained by the fact that the inclusion of alternative conformations is more difficult for fragments of the main chain than for side chains. As a consequence, the number of AC fragments in the main chain is highly underestimated in PDB structures. This causes growth of both the false-positive and false-negative rates, as discussed in §4.1. Slightly worse results for the prediction of outer side chains compared with the inner side chains can be explained by the fact that fully disordered residues (included in the model as SC) are mostly located on the surface of the molecule.

We tested five decision-making procedures and obtained similar prediction qualities for all of them. The prediction accuracy achieved at present does not provide a reason to decide on any of the tested procedures. Generally, the quality of prediction approximately matches the results of CASP competitions devoted to 'identifying disordered regions in target proteins'.

4.4. Low-resolution and high-resolution structures

The main part of the research was conducted at atomic resolution (1.2 Å and better) because it is known that at this resolution the ordered part of a structure is stable in unrestrained refinement. A similar prediction quality can also be obtained for higher resolutions. Table 5 presents the results of evaluation of decision-making procedures when working at resolutions higher than 1.1 Å (database 2, test sample).

If the resolution of the X-ray data is worse than 1.2 Å the application of decision-making procedures becomes more complicated. Firstly, at this resolution all atoms change their positions significantly and it becomes difficult to distinguish AC atoms from SC atoms from their shifts. Another problem is that at lower resolution alternative conformations are not so clearly visible in electron-density maps and are rarely included in the model. This significantly spoils the database and makes it difficult both to derive the procedure parameters and to evaluate the procedure quality. Diagrams of atomic shifts may be still useful because they highlight the relatively high shifts that are usual for residues that possess alternative conformations or are disordered. Our tests have shown that automated analysis of atomic shifts in unrestrained refinement becomes confusing when applied at resolutions much worse than approximately 1.2 Å. Nevertheless, some modification of the approach could possibly extend it to a lower resolution zone. Recently, Pozharski (2011) has shown increased mobility of disordered residues in refinement even when stereochemical restraints are retained. This indicates the possibility of looking for decision-making procedures based on shifts of atoms in restrained refinement at medium resolution.

4.5. Decision-making procedures based on ADP and electron-density values

Atomic shifts are not the only feature that allows judgement of whether a residue is present in a single conformation or in alternative conformations. The usual practice is to estimate the degree of disorder in the structure from the values of the isotropic atomic displacement parameters (B values) that are calculated as the outcome of any refinement program. A decision-making procedure based on analysis of ADP values

can be constructed and tested in a similar way to that used for atomic shifts. The only difference is that an averaged ADP value for a residue is now compared with some threshold derived from a database or probabilities are calculated and compared with such an averaged ADP value for different types of residues.

A similar comparison was made for one further parameter that can be used as an indicator of disorder. In this test, we analyzed the values of electron density at atomic centres in $2mF_{obs} - DF_{calc}$ syntheses calculated with *phenix.model_vs_data* from the models obtained in the first stage of database preparation (§2.4). ROC curves corresponding to decision-making procedures based on atomic shifts, ADPs and density values are shown in Fig. 9.

The comparison shows that although the *B* values and density values show some predictive power, the best prediction quality is achieved with procedures based on analysis of the atomic shifts. Pearson's correlation coefficient calculated between the atomic shifts and ADP or density values was found to be 0.537 and −0.414, respectively, when using database 1. The negative value of the second correlation coefficient reflects the fact that poorly ordered atoms have large shifts and ADP values but small density values.

4.6. The use of different refinement programs

Different programs for crystallographic refinement have their own internal procedures for stabilizing the refinement that affect the values of the atomic shifts obtained. Therefore, the values of the thresholds and the empirical probability distributions for different types of atoms are specific to a particular refinement program. The tendency to have large values of shifts for atoms occupying alternate positions also occurs in other programs. As a result, the diagrams of atomic shifts are more software-independent and can be used to analyze the output of any refinement program. In this study,
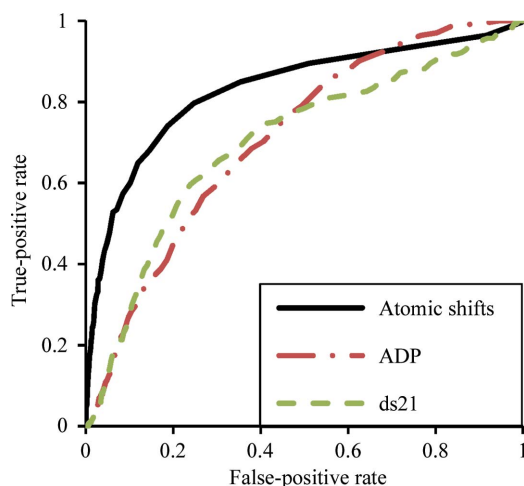
we used the *PHENIX* suite because it provides a good opportunity to automate the processing of the PDB data.

5. Conclusion

Trial unrestrained refinement followed by an analysis of atomic shifts highlights the most unstable parts of the structure. These parts are prime candidates for the introduction of alternative conformations and should be tested first with electron-density maps. The proposed formal decision-making procedures do not allow prediction of exactly which residues are present in alternative conformations, but provide an opportunity to reduce the amount of work required for visual analysis of the maps, identifying the most likely candidates. Decision-making procedures based on analysis of atomic shifts have shown greater predictive power than more straightforward approaches based on ADP values or point electron-density values. Further improvement of the quality of predictions can be achieved by constructing more accurate training samples and by combining different methods of prediction. In its current implementation, the method is applicable at resolutions better than 1.2 Å. Application of the method at worse resolutions is problematic and requires further improvements.

In the framework of this research, several programs were developed for database processing, plotting diagrams of atomic shifts and the application and evaluation of decision-making procedures. They are available from http://www.impb.ru/lmc/programs/ac_prediction/ or from the authors on request.

Figure 9
ROC curves for the decision-making procedure based on the mean shift ('atomic shifts'; black solid line), ADP values ('ADP'; green dashed line) and $2mF_o - DF_c$ electron density ('ds21'; red dotted–dashed line) (side inner residues, database 1, test sample, $0.0961 \leq R_{work} \leq 0.1278$).

References

Adams, P. D. *et al.* (2010). *Acta Cryst.* D**66**, 213–221.
Addlagatta, A., Krzywda, S., Czapinska, H., Otlewski, J. & Jaskolski, M. (2001). *Acta Cryst.* D**57**, 649–663.
Afonine, P. V., Grosse-Kunstleve, R. W., Chen, V. B., Headd, J. J., Moriarty, N. W., Richardson, J. S., Richardson, D. C., Urzhumtsev, A., Zwart, P. H. & Adams, P. D. (2010). *J. Appl. Cryst.* **43**, 669–676.
Afonine, P. V., Grosse-Kunstleve, R. W., Echols, N., Headd, J. J., Moriarty, N. W., Mustyakimov, M., Terwilliger, T. C., Urzhumtsev, A., Zwart, P. H. & Adams, P. D. (2012). *Acta Cryst.* D**68**, 352–367.
Antson, A. A., Smith, D. J., Roper, D. I., Lewis, S., Caves, L. S., Verma, C. S., Buckley, S. L., Lillford, P. J. & Hubbard, R. E. (2001). *J. Mol. Biol.* **305**, 875–889.
Berman, H. M., Westbrook, J., Feng, Z., Gilliland, G., Bhat, T. N., Weissig, H., Shindyalov, I. N. & Bourne, P. E. (2000). *Nucleic Acids Res.* **28**, 235–242.
Dauter, Z., Sieker, L. C. & Wilson, K. S. (1992). *Acta Cryst.* B**48**, 42–59.
Dodd, F. E., Hasnain, S. S., Abraham, Z. H. L., Eady, R. R. & Smith, B. E. (1995). *Acta Cryst.* D**51**, 1052–1064.
Fawcett, T. (2006). *Pattern Recognit. Lett.* **27**, 861–874.

Getzoff, E. D., Gutwin, K. N. & Genick, U. K. (2003). *Nature Struct. Biol.* **10**, 663–668.

Howard, E. I., Sanishvili, R., Cachau, R. E., Mitschler, A., Chevrier, B., Barth, P., Lamour, V., Van Zandt, M., Sibley, E., Bon, C., Moras, D., Schneider, T. R., Joachimiak, A. & Podjarny, A. (2004). *Proteins*, **55**, 792–804.

Kabsch, W. & Sander, C. (1983). *Biopolymers*, **22**, 2577–2637.

Koepke, J., Scharff, E. I., Lücke, C., Rüterjans, H. & Fritzsch, G. (2003). *Acta Cryst.* D**59**, 1744–1754.

Kursula, I. & Wierenga, R. K. (2003). *J. Biol. Chem.* **278**, 9544–9551.

Moriarty, N. W., Grosse-Kunstleve, R. W. & Adams, P. D. (2009). *Acta Cryst.* D**65**, 1074–1080.

Morris, R. J. & Bricogne, G. (2003). *Acta Cryst.* D**59**, 615–617.

Noivirt-Brik, O., Prilusky, J. & Sussman, J. L. (2009). *Proteins*, **77** Suppl. S9, 210–216.

Pozharski, E. (2011). *Acta Cryst.* D**67**, 966–972.

Rypniewski, W., Østergaard, P., Nørregaard-Madsen, M., Dauter, M. & Wilson, K. S. (2001). *Acta Cryst.* D**57**, 8–19.

Ševčík, J., Dauter, Z. & Wilson, K. S. (2004). *Acta Cryst.* D**60**, 1198–1204.

Sheldrick, G. M. (1990). *Acta Cryst.* A**46**, 467–473.

Sobolev, O. V. (2008). *International School of Crystallography, 40th Course, Erice, Italy: Programme, Lecture Notes and Poster Abstracts*, p. 384.

Sobolev, O. V. & Lunin, V. Y. (2008). *Math. Biol. Bioinf.* **3**, 50–59.

Wang, J., Dauter, M., Alkire, R., Joachimiak, A. & Dauter, Z. (2007). *Acta Cryst.* **63**, 1254–1268.